

## Scanning Probe Microscopy in Technology of Solar Cells Production

B. Mojrová<sup>1</sup>, P. Bařinková<sup>2</sup>, J. Boušek<sup>1</sup>, O. Hégr<sup>1</sup>, R. Bařinka<sup>2</sup>, J. Hofman<sup>1</sup>

<sup>1</sup>Department of Microelectronics, Faculty of Electrical Engineering and Communication,  
Brno University of Technology,  
Technická 3058/10, Brno

<sup>2</sup>Fill factory s.r.o.,  
Televizní 2618, Rožnov pod Radhoštěm

E-mail : xmojro00@stud.feec.vutbr.cz, pavlina.barinkova@fillfactory.cz

### Abstract:

This article deals with implementation of Scanning Probe Microscopy (SPM) techniques to the characterization of crystalline silicon solar cells. Atomic Force Microscopy (AFM) is used for the characterization of solar cells texture, because it allows three dimensional imaging of surface structure [1]. Aim of this part of work was to set up a new methodology for surface evaluation in terms of optimization of the texturing process in solar cells mass-production. Monocrystalline silicon (mono-Si) wafers were etched in strong and weak alkaline solutions, and in strong acid solution which corresponds to standard methods of solar cells production. A detailed description of the surface was based on inspection of roughness parameters which were determined by the analysis of surface images.

The second part of this work deals with possibility of Kelvin Probe Force Microscopy (KPFM) application for detection of Back Surface Field (BSF) presence and measurement its depth. KPFM enables to image surface electronic properties – specifically the Contact Potential Difference ( $U_{CPD}$ ) [2]. This method was used for checking the aluminum BSF (Al-BSF) layer presence and for measuring its depth.

## INTRODUCTION

The characterization of surface properties is a very important part of the crystalline silicon solar cell production. Some properties can be ascertained using SPM techniques. For textured surface analysis the AFM was chosen, because this method allows a three-dimensional visualization of conductive, semi-conductive and non-conductive samples topography. The AFM is based on force interactions between the surface and the silicon-nitride tip, which scans the whole sample surface. The resolution is then determined only by tip sharpness and scan velocity [1] [3].

The AFM was used for invent a way of evaluation of the textured surface of the silicon substrate, and to test it afterwards. So far used methods, the optical microscopy and the visual inspection, depend very much on practical experience of an assessing person. KPFM is a SPM method that enables imaging of the surface electric properties using contact potential difference between the tip and the sample. This method can be applied for thickness measurement of various layers or determination of layer presence and homogeneity [2] [4].

Due to the high spatial resolution, this method was used for checking the aluminum BSF (Al-BSF) layer presence and for measuring its depth and gradient in the doping level.

The experiments were conducted in the laboratories of Fill factory s.r.o. using the NTEGRA Prima microscope provided by NT/MDT, with modification

for scanning the samples. The image evaluation was done by the Gwyddion program [6] and selected roughness parameters were used for surface describing.

## ANALYSIS OF SURFACE TOPOGRAPHY BY AFM

### Surface texturing

In the typical manufacturing process flow texturing process is done before the diffusion process. The standard process of surface texturing is accomplished in two steps. The first step is saw damage removal to remove a layer (usually 5 – 10  $\mu\text{m}$ ) with most of defects and impurities. Due to easier waste disposal alkaline etching solutions of potassium hydroxide (KOH) or sodium hydroxide (NaOH) are preferred to acidic etching solutions. Saw damage removal by acidic solution enables an isotropic etching, which is preferred for multicrystalline substrates [4].

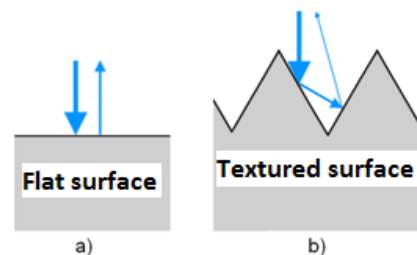


Fig. 1: Effect of surface texturing [8]

The wafer surface after saw damage removal is very glossy and it reflects a large amount of light (more than 35 % of incident light). The second step, texturing is done due to a light reflection reduction and to increase the absorption efficiency (see Fig. 1: Effect of surface texturing) [6].

Type of the etching solution, its composition and process conditions affect texture properties very significantly. Texturing is done by the etching in strong alkaline or acidic solutions. The silicon etching rate in strong alkaline solutions (NaOH or KOH) depends on crystallographic orientation of silicon substrate. Because the etching is faster in  $\langle 100 \rangle$  direction than  $\langle 111 \rangle$  direction, a typical pyramidal structure for monocrystalline substrate is created. Size of these square-base pyramids is adjusted to a few microns. [4].

### Sample preparation

For experiments mono-Si substrates were used due to the same crystallographic orientation in the whole sample. The orientation was  $\langle 100 \rangle$  in all cases. A list of samples and etching parameters are given in the table 1. Both SDE samples were etched in a strong KOH solution used for saw damage removal, TAI samples in a weak NaOH solution used for standard pyramid texturing. The sample TAc 1 was etched in a mixture of hydrofluoric acid (HF), nitric acid (HNO<sub>3</sub>), phosphoric acid (H<sub>3</sub>PO<sub>4</sub>), and acetic acid (CH<sub>3</sub>COOH). The acid mixture for etching the sample TAc 2 was composed of HF, HNO<sub>3</sub>, H<sub>3</sub>PO<sub>4</sub>, and sulfuric acid (H<sub>2</sub>SO<sub>4</sub>). A surface reflection was determined by the visual comparison of samples.

Table 1: Overview of samples measured by AFM

<i>Sample</i>	<i>Etching process</i>	<i>Etching solution</i>	<i>Reflection</i>
SDE 1	Saw damage removal	KOH solution	High
SDE 2	Saw damage removal	KOH solution	High
TAI 1	Alkaline texturing	NaOH solution	Low
TAI 2	Alkaline texturing	NaOH solution	Low
TAc 1	Acidic texturing	HF + HNO <sub>3</sub> + H <sub>3</sub> PO <sub>4</sub> + CH <sub>3</sub> COOH	Medium
TAc 2	Acidic texturing	HF + HNO <sub>3</sub> + H <sub>3</sub> PO <sub>4</sub> + H <sub>2</sub> SO <sub>4</sub>	Low

Because SPM methods measure only surface properties, it was necessary to clean samples before measurement. Wafers after etching processes were broken into pieces, which were fixed to pads and then thoroughly cleaned with compressed air.

### Surface analysis

To compare images each other a uniform size of a scanned area, image resolution and scanning velocity must be assessed. The resolution was set up to  $256 \times 256$  point. The width of the scanned area must be large enough to enable a clear depiction of the given surface. This size was set at  $50 \times 50 \mu\text{m}$ , based on the measurements. Scanning frequency, in case of this device, should not exceed  $f_{scanning} = 0,2 \text{ Hz}$ , so the velocity was given at  $v_{scanning} = 20 \mu\text{m/s}$ . All samples were measured in a semicontact mode [8].

The roughness parameters are most commonly used for the characterization of the surface with a non-periodic structure. First it was necessary to establish basic requirements for textured surface properties. A high value of surface roughness and a high profile inclination is demanded for the surface of the solar cell front side. Surface waviness is related with a size of etched objects. Shallower etch pits and therefore the lower value of waviness is desirable. Otherwise deep etch pits (so called underetching) may locally weakening of the substrate which is then prone for breakages [9] [10].

On the ground of the above mentioned requirements following parameters were chosen to describe the shape and the depth of etched object: the root mean square deviation of roughness  $R_q$ , the root mean square deviation of waviness  $W_q$ , and the root mean square slope of roughness  $R_{Aq}$ .

Amplitude parameters (in this case  $R_q$  and  $W_q$ ), defined in the Z axis, are determined only by peak heights and valley depths or their combination without regard to their proportions in a horizontal direction [9]. Root mean square deviation from the assessed profile (i.e.  $R_q$  and  $W_q$ ) is the root mean square value of the ordinate values  $R_{(x)}$  or  $W_{(x)}$  within the sampling length. Root mean square parameter gives extra weight to the numerically higher values of surface height in contrast to arithmetic average [11]. Root mean square slope of the ordinate slopes  $dZ/dX$  within the sampling length (i.e.  $R_{Aq}$ ) depends on both amplitude and spacing and is therefore a hybrid parameter [11]. The  $R_{Aq}$  is very sensitive to all extraordinary values of local slopes and therefore it is very often used for analysis of optical devices surface [9].

The Gwyddion program enables an evaluation of standardized roughness parameters according to ISO 4287-1997, and ISO 4287/1-1997 [6].

The Fig. 2: Images of silicon surface shows surface structures of mono-Si substrates after etching processes. The roughness parameters were determined in three selected sections which covered the most significant objects of the image. The average value for each parameter and sample are in the table 2, statistic representation of measured values is given on Fig. 3: Statistic representation of ascertained values of roughness parameters.

Table 2: Average values of roughness parameters obtained by image analysis by Gwyddion program

Sample	$R_q$ [ $\mu\text{m}$ ]	$W_q$ [ $\mu\text{m}$ ]	$R_{Aq}$ [-]
SDE 1	0,089	2,275	$2,02 \cdot 10^{-4}$
SDE 2	0,068	1,481	$1,54 \cdot 10^{-4}$
TAI 1	0,294	1,866	$6,65 \cdot 10^{-4}$
TAI 2	0,406	3,097	$9,16 \cdot 10^{-4}$
TAc 1	0,133	2,181	$3,00 \cdot 10^{-4}$
TAc 2	0,257	1,486	$5,81 \cdot 10^{-4}$

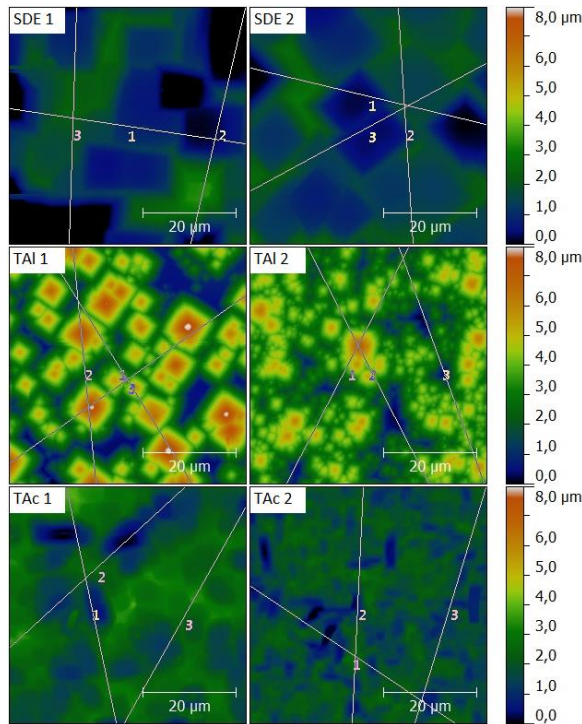


Fig. 2: Images of silicon surface after: saw damage removal in weak alkaline solution of KOH (SDE 1 and SDE 2); texturing in strong alkaline solution of NaOH (TAI 1 and TAI 2); texturing in acid solutions (TAc 1 and TAc 2)

It is obvious that the chosen size of the scanned area gives a clear picture of surface topography. In both cases of acid texturing a presence of underetching is seen. The difference in a surface structure between samples after the same etching process is caused by different etching conditions.

Surfaces after saw damage removal (SDE 1 and SDE 2) reflected most of the light and the average values of  $R_q$  and  $R_{Aq}$  are the lowest, according to the assumption mentioned above. In the image of mono-Si substrate with the alkaline texture (TAI 1) typical pyramids are shown evenly distributed over the entire surface. The light reflectance of these samples was considerably much lower than of the substrate after saw damage removal. This corresponds to the highest values of  $R_q$  and  $R_{Aq}$ . The light reflectance was also low in case of sample TAc 2 with acidic texture.

The sample TAc 1 reflected more light than substrates with alkaline texture, but less than substrate after saw damage removal and thus the  $R_q$  and  $R_{Aq}$  values are slightly higher. The  $W_q$  parameter

indicates a surface evenness – surface with homogeneity structure (e.g. SDE 2, TAI 1, and TAc 2) have smaller values of  $W_q$  than the other samples. The high  $W_q$  value of sample is caused by deep etch pits.

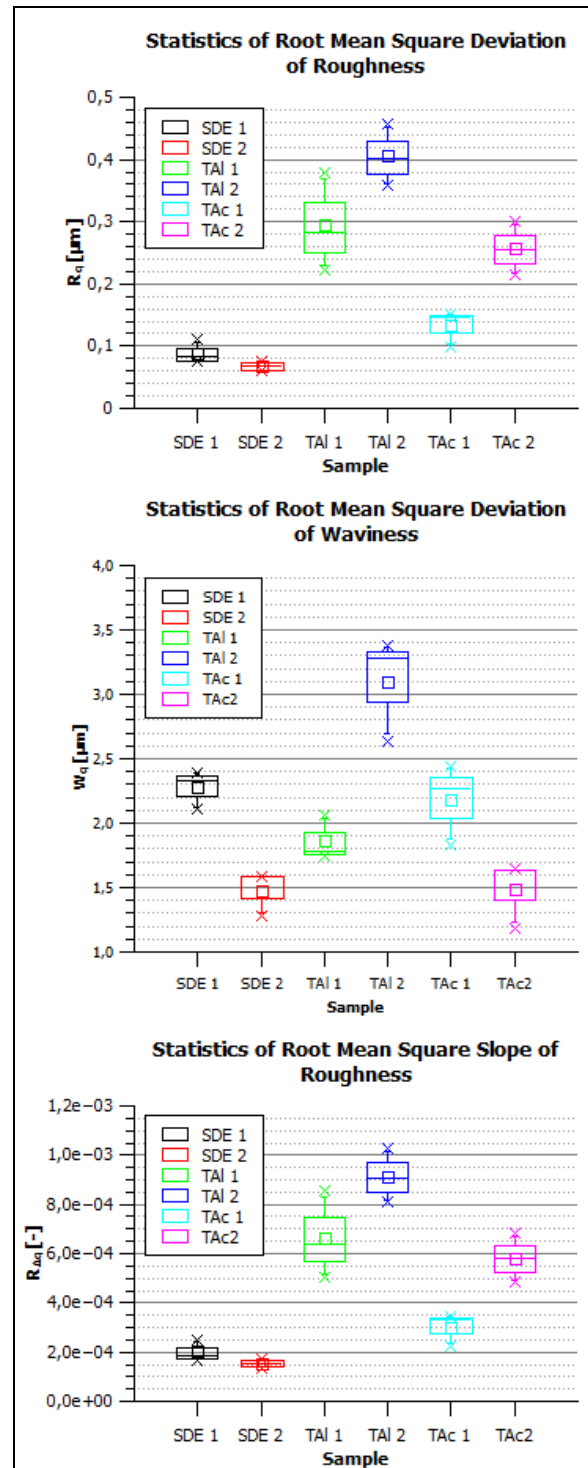


Fig. 3: Statistic representation of ascertained values of roughness parameters

# MEASUREMENT OF ALUMINIUM BACK SURFACE FIELD BY KPFM

## Back Surface Field

To minimize the surface recombination a thin and a high level doping region is usually formed on the rear side of the solar cell. This  $p^+-p$  (for  $p$ -type substrate) junction is also known as a Back Surface Field (BSF). It works as an electrical mirror and it keeps minority carriers away from the back ohmic contact (see Fig. 4: Schematic illustration of Al-BSF function). BSF formation can be done by the diffusion of boron but in industry a full-area Al-BSF is used in most cases. Another option of BSF formation is presence of the fixed charge appropriate polarity in the passivation layer [11] [13].

The Al-BSF provides an ohmic contact and a moderate rear surface passivation with typical effective rear surface recombination velocities  $S_{rear}$  ranging from 200 cm/s to 600 cm/s on 1-3  $\Omega \cdot \text{cm}$   $p$ -type silicon [14].

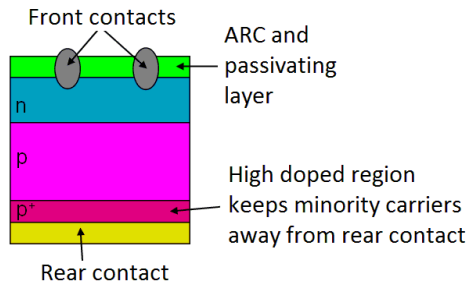


Fig. 4: Schematic illustration of Al-BSF function [8]

The  $p^+$  region in case of Al-BSF is usually created by screen-printing aluminum paste following by drying to vaporize the organic solvents in the aluminum paste, and high temperature sintering ( $700^\circ\text{C} - 900^\circ\text{C}$ ) in a belt furnace. During heating up thin silicon layer is dissolved in the liquid phase and aluminum is then dissolved in it. A recrystallization of liquid alloy to solid solution, containing silicon and aluminum, is under way during the rapid cooling down. This solid solution creates a thin  $p^+$  type layer, where approximately 12% of silicon is presented [14].

## Sample preparation

For this experiments were used standard solar cells from monocrystalline  $p$ -type silicon wafers with the  $\langle 100 \rangle$  crystallographic orientation. The standard process means saw damage removal in a KOH solution, texturing in a NaOH solution, phosphorous diffusion, and deposition of a silicon nitride ( $\text{SiN}_x$ ) as an antireflection and passivating layer. An aluminum paste used for BSF formation was deposited by screen printing on the rear side and then fired. In order to investigate the  $p^+$  layer, the aluminum layer was removed from the  $p^+$  type region by etching in HCl solution. The last step was cross sectioning of the sample by cutting machine and cutting to small

pieces. Afterwards samples were fixed to pads with contact and then thoroughly cleaned with compressed air.

## Al-BSF measurement

KPFM is a double pass method. During the first pass the sample topography is ascertained by AFM measurement. In this case a semicontact mode was used. The tip is subsequently lift up 10 nm above the surface and contact potential difference is measured. A list of samples and scanning parameters is given in the table 3.

Table 3: Overview of samples measured by KPFM

Sample	Scan size [ $\mu\text{m}$ ]	Step size [nm]	$V_{scanning}$ [ $\mu\text{m/s}$ ]
BSF 1	$40,89 \times 15,9$	250	6,4
BSF 2	$20,04 \times 5,52$	78,43	8,044

All samples were measured in the direction from the centre to the edge of sample for the purpose of good depiction of the edge. The scanning direction on the Fig. 6: Images of contact potential difference represents the probe motion in the course of one line scanning. This direction was changed in the case of the sample BSF 2 in order to better imaging the  $U_{CPD}$ , because it comes about to worn out of a conductive layer on the tip in the course of scanning.

Because the  $U_{CPD}$  was measured on the edge of the sample which is not straight, it was necessary to find out the real edge of sample. For this reason the topography images were used. The  $U_{CPD}$  profiles (see Fig. 7: Profiles of contact potential difference) were ascertained afterward.

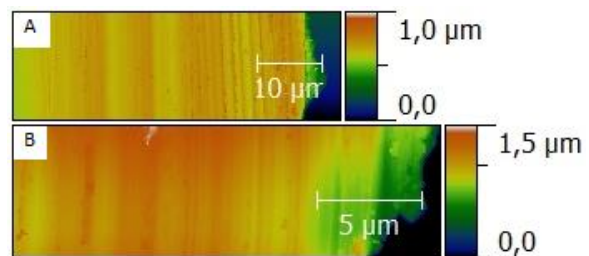


Fig. 5: Images of topography of BSF 1 (A) and BSF 2 (B)

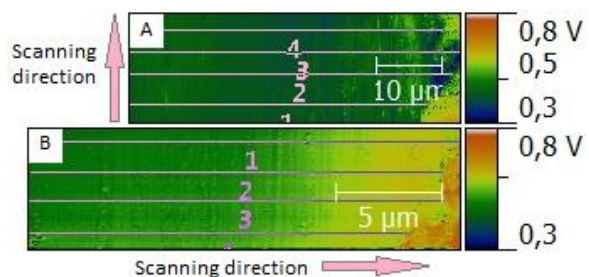


Fig. 6: Images of contact potential difference  $U_{CPD}$  measured on sample BSF 1 (A) and BSF 2 (B) with marked scanning directions and position of profiles

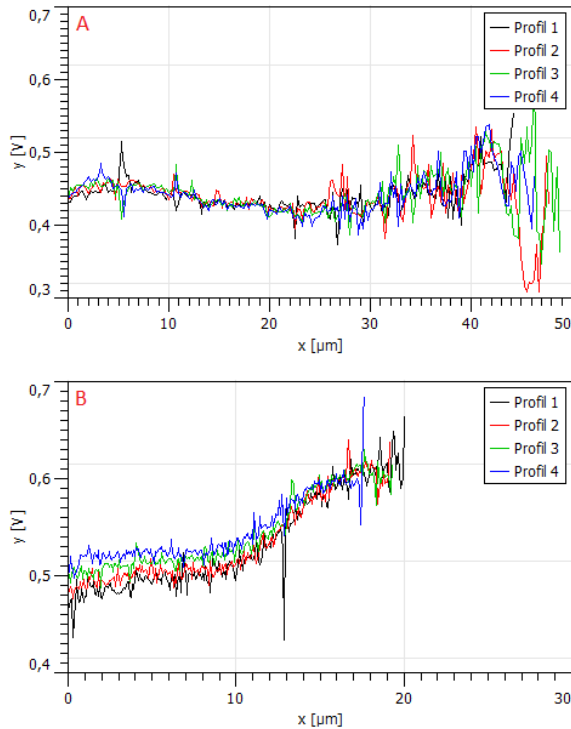


Fig. 7: Profiles of contact potential difference  $U_{CPD}$  measured on sample BSF 1 (A) and BSF 2 (B)

Table 4:  $U_{CPD}$  values and Al-BSF size

Sample	$U_{CPD-Peak}$ [V]	$U_{CPD-Si}$ [V]	$d_{Al-BSF}$ [ $\mu m$ ]
BSF 1	0,52	0,43	4,5
BSF 2	0,60	0,50	6,5

For each sample two average values from  $U_{CPD}$  profile measurements were obtained (highest value  $U_{CPD-Peak}$ , which belongs to the Al-BSF layer, and  $p$  type silicon  $U_{CPD-Si}$ ), and they are given in the table 4. At the same time an assumed thickness of Al-BSF was measured from the profiles.

From the Fig. 6: (B) and the Fig. 7: (B) it is obvious, that Al-BSF layer presence and thickness can be observed with the sample BSF 2. In this case an expected Al-BSF thickness  $d_{Al-BSF}$  is around 6,5  $\mu m$  (see the table 4). In spite of the fact that the surface topography of the sample BSF 1 affects  $U_{CPD}$  image (see the Fig. 5: (A) and the Fig. 6: (A)), it is possible to determine the Al-BSF presence. The scanning direction used for the sample BSF 2 seems to have a smaller influence of the topography. To achieve a better  $U_{CPD}$  image it is necessary to use another method for cross sectioning.

## CONCLUSIONS

The first part of this work illustrates the using of atomic force microscopy in the crystalline silicon solar cell production. Based on the measurements a methodology for assessment of silicon surface properties after etching process was suggested. This method allows obtaining a description of different morphologies of selected surfaces. The selected size

of captured area, using the AFM, shows clear images of the surface structure, which was impossible using the usual methods. The texture homogeneity and a presence of underetching can be observed.

The chosen parameters of roughness  $R_q$ ,  $W_q$ , and  $R_{Aq}$  enable the description of surface structure and it has been proven, that there is a connection with the optic properties of the substrate. The parameters can be also used for setting up and controlling the etching process.

The second part of this work deals with using of Kelvin probe force microscopy to measurement aluminum back surface field properties. From experiments it is obvious that KPFM allows imaging of Al-BSF so it is possible to measure Al-BSF depth.

## ACKNOWLEDGEMENTS

This work was done in the frame of the project FR-T11/599 supported by Ministry of Industry and Trade of the Czech Republic within the program TIP 2009, European project 7D-12002 within the program Eurostars E!6404 – Solar Team, and by project no. FEKT-S-14-2300 A new types of electronic circuits and sensors for specific applications.

## REFERENCES

- [1] Machala, T., Vůjtek, M., Kubínek, R. at al., Mikroskopie skenující sondou [online], UPOL, 2003 [cit. 2014-09-30]. Available from WWW: <<http://atmilab.upol.cz/mss/>>.
- [2] Sadewasser S. and Glatz. T., Kelvin Probe Force Microscopy. London, Springer Science & Business Media, 2012.
- [3] Bowen, W. R., Hilal N., Atomic Force Microscopy in Process Engineering. Oxford, Elsevier Ltd., 2009.
- [4] Melitz, W. at al., "Kelvin Probe Force Microscopy and its Application," Surface Science Reports, vol. 66, pp. 1-27, January 2011.
- [5] Solanski, C. S., Solar Photovoltaics: Fundamentals, Technologies and Applications. New Delhi, PHI Learning Pvt. Ltd., 2011.
- [6] Nečas, D. Gwyddion: an open-source software for SPM data analysis, ver. 2.33 [software]. Brno, 2013 [cit. 2014-09-30]. Available from WWW: <<http://gwyddion.net/>>.
- [7] Markvart, T., Castaner, L., Practical Handbook of Photovoltaics: Fundamentals and Applications. Oxford, Elsevier Science Ltd., 2003.
- [8] Mojrová, B., Využití měřící metody SPM v technologii výroby krystalických solárních článků - master's thesis, Brno, FEKT VUT, 2013.

- [9] Novák, Z., "Zvýšení kvality hodnocení textury povrchu," MM Průmyslové spectrum [online], vol. 11, pp. 52-54, 2011.
- [10] Bařínková P., Analýza morfologie povrchu a její využití při optimalizaci procesu úpravy povrchu křemíkového substrátu za účelem zajištění vhodných optických a elektronických parametrů pro výrobu solárních článků. Rožnov pod Radhoštěm, 2012.
- [11] ČSN EN ISO 4287, Geometrické požadavky na výrobky (GPS) – Struktura povrchu: Profilová metoda – Termíny, definice a parametry struktury povrchu. Praha, 1999.
- [12] Luque, A., Hegedus, S., Handbook of Photovoltaics science and engineering, Chichester, John Wiley & Sons, Ltd, 2003.
- [13] Goetzberger, A. at al., Crystalline Silicon Solar Cells, Chichester, John Wiley & Sons, Ltd, 1998.
- [14] Peters, S., Rapid Thermal Processing of Crystalline Silicon Materials and Solar Cells – Ph.D. thesis, Konstanz, Universität Konstanz, 2004.